Check for updates

ADVANCING EARTH AND SPACE SCIENCE

Geophysical Research Letters

RESEARCH LETTER

10.1029/2021GL095476

Key Points:

- Van Allen Probes and ground-based sites observed correlated periodic very low-frequency emissions with periods of 2 or 4 s consistent with wave bouncing
- Poynting flux directions at Van Allen Probes were opposite in neighboring pulses in one regime and parallel in the other regime
- The pulse period onboard the spacecraft was half of that on the ground in the first regime and the periods were equal in the second regime

Correspondence to:

A. G. Demekhov,
andrei@ipfran.ru

Citation:

Demekhov, A. G., Titova, E. E., Manninen, J., Nikitenko, A. S., & Pilgaev, S. V. (2021). Short periodic VLF emissions observed simultaneously by Van Allen Probes and on the ground. *Geophysical Research Letters*, *48*, e2021GL095476. https://doi.org/10.1029/2021GL095476

Received 3 AUG 2021
Accepted 5 OCT 2021

© 2021. American Geophysical Union. All Rights Reserved.

Short Periodic VLF Emissions Observed Simultaneously by Van Allen Probes and on the Ground

A. G. Demekhov[1,2], E. E. Titova[1,3], J. Manninen[4], A. S. Nikitenko[1], and S. V. Pilgaev[1]

[1]Polar Geophysical Institute, Apatity, Russia, [2]Institute of Applied Physics of the Russian Academy of Sciences, Nizhny Novgorod, Russia, [3]Space Research Institute of the Russian Academy of Sciences, Moscow, Russia, [4]Sodankylä Geophysical Observatory, Sodankylä, Finland

Abstract We present simultaneous observations of very low-frequency emissions with periodic bursts by Van Allen Probe near geomagnetic equator and Kannuslehto and Lovozero ground-based sites. The repetition period and ground–spacecraft delay are consistent with guided whistler wave propagation between conjugate ionospheres. In contrast to lightning whistlers, the group velocity dispersion is not accumulated from one burst to another, thus implying a nonlinear mechanism of its compensation. Two regimes are observed. In one regime, Poynting flux direction alternates in the magnetosphere, and the burst period (2 s) is half of that detected on the ground (4 s), corresponding to single-wave packet bouncing along the field line. This regime is switched to the other one, with burst period unchanged in the magnetosphere but halved on the ground. In this second regime, no alternating Poynting flux direction is observed. The second regime corresponds to two symmetrically propagating wave packets synchronously meeting at the equator.

Plain Language Summary The near-Earth space is populated by energetic charged particles (ions and electrons) forming radiation belts and ring current and having energies from several keV to several MeV. Energetic particles can damage spacecraft electronics and affect the health of humans in space. Recently, the radiation belt dynamics attracted great interest among researchers and new spacecraft research missions have been launched for these studies. Dynamics of radiation belt electrons is to a great extent determined by energetic particle interaction with very low-frequency (VLF) electromagnetic waves (~10^3–10^4 Hz). These waves can propagate from one hemisphere to the other along geomagnetic field lines, and characteristic propagation times are 1–5 s depending on the latitude and plasma density. We study a distinct type of VLF emissions whose amplitude is periodically modulated with periods of several seconds (periodic emissions). In contrast to previous studies using ground-based data, we use simultaneous observations by Van Allen Probe in the equatorial magnetosphere and ground stations. Our analysis allowed us to show for the first time that the modulation period of these emissions is related to the wave propagation time between conjugate hemispheres. We observed two regimes corresponding to a single-wave packet or two symmetrically propagating wave packets.

1. Introduction

Very low frequency (VLF) emissions in the magnetosphere are often observed in the form of periodic or quasiperiodic sequence of bursts. Helliwell (1965) termed periodic emissions (PE) as the bursts having repetition periods of 3–10 s consistent with individual wave packet propagation between conjugate ionospheres. This period can be very stable in time for long time intervals. Quasi-periodic (QP) emissions have longer periods (usually from 20–30 to 300 s), and the inter-element interval can vary smoothly due to several factors (Manninen et al., 2014).

Such events can last tens of minutes and even several hours (Manninen et al., 2014), which require the amplification of whistler mode waves in the magnetosphere to compensate for the losses due to nonideal ionospheric reflection and refractive spreading of wave energy. The commonly accepted amplification mechanism of whistler mode waves in the inner magnetosphere is cyclotron resonant interaction with energetic electrons having anisotropic velocity distribution (Trakhtengerts & Rycroft, 2008).

Periodic emissions are divided into two subtypes, which Helliwell (1965) termed as dispersive and non-dispersive. The period of dispersive PE has a systematic frequency-time dispersion typical of multi-hop whistler-mode waves. The period of nondispersive PE does not change with frequency, that is, the effect of group velocity dispersion is not accumulated from pulse to pulse and successive wave packets have the same shape on the dynamical spectrogram.

Engebretson et al. (2004) demonstrated a transition of echoing whistlers to PE and then to QP emissions. Manninen et al. (2014) were able to reliably associate PEs observed inside QP emissions with the two-hop whistler mode period. Both papers suggested that PEs were generated in a localized region, in the outer plasmasphere/plasmapause.

The observations of PEs at conjugate stations (Lokken et al., 1961) showed that the emissions appeared alternately at the two stations with a time delay of about one-hop whistler transit time. Helliwell (1963) and Helliwell and Brice (1964) observed events in which the periods of dispersive and nondispersive PEs and the whistler-mode two-hop group delay were the same. This led to a suggestion that the subsequent periodic elements (bursts) may be triggered by the previous ones (Helliwell, 1963, 1965). Another mechanism of PE generation proposed by Dowden (1962) is related to the period of charged particle bouncing between conjugate hemispheres.

An advanced theoretical model of nondispersive PE was developed by Bespalov (1984). The model is based on a passive mode locking regime in the cyclotron instability in which the group velocity dispersion is compensated by quasi-linear modification of the energetic electron distribution function. However, this model assumes that electron bounce periods are much shorter than the whistler hop scales. Overall, the PE phenomenon remains poorly studied.

Most PEs have been observed by ground-based instruments. Two examples of PE observations by a low-orbiting DEMETER spacecraft have been reported by Bespalov et al. (2010). In this paper, we present the first report of conjugate detection of PE on the ground and onboard magnetospheric spacecraft.

2. Instruments and Data

Van Allen Probes (earlier Radiation Belt Storm Probes) are two identical spacecraft that had low-inclination (10°) orbits with 600 km perigee and 30,000 km apogee (Mauk et al., 2012). Wave measurements were made by the Electric and Magnetic Field Instrument Suite and Integrated Science (EMFISIS) (Kletzing et al., 2013).

In this paper, we use the data of waveform (WFR) and high-frequency (HFR) receivers. The WFR comprises a six-channel waveform receiver, simultaneously samples all three electric and all three magnetic components of waves in the frequency range of ~10 Hz to 12 kHz with a 35 kHz sampling rate and 16 bits of digitization. The waveforms are recorded during 6-s intervals.

Plasma density was obtained from HFR spectra by using the upper hybrid resonance (UHR) line (Kurth et al., 2015).

Ground-based observations of VLF signals were carried out in Northern Finland at Kannuslehto (KAN, 67.74°N, 26.27°E; L = 5.51) and Lovozero (LOZ, 67.98°N, 35.08°E; L = 5.54). The distance between KAN and LOZ is 400 km. The measurements are performed by two orthogonal vertical magnetic loop antennas oriented in the north-south and east-west directions and by a vertical electric field sensor installed at LOZ. Electric field measurements allow us to resolve the 180° ambiguity in the Poynting flux direction. More detailed descriptions of the hardware are given in (Fedorenko et al., 2014; Manninen, 2005).

3. Observations

3.1. Overview of the Event

We consider the event of March 03, 2019. Periodic emissions were observed from 15:35 to 17:05 UT at KAN and LOZ and from 15:51 to 17:07 UT at Van Allen Probe A (VAP-A). During this event, VAP-A was near the equator (MLAT varied from 0.5° to −0.5° and MLT from 17.4 to 18.2). The waveforms were recorded by EMFISIS for two adjacent 6-s intervals every 4 min. The geomagnetic activity during the PE observations was low: $K_p = 1-$, $D_{st} = -11$ nT.

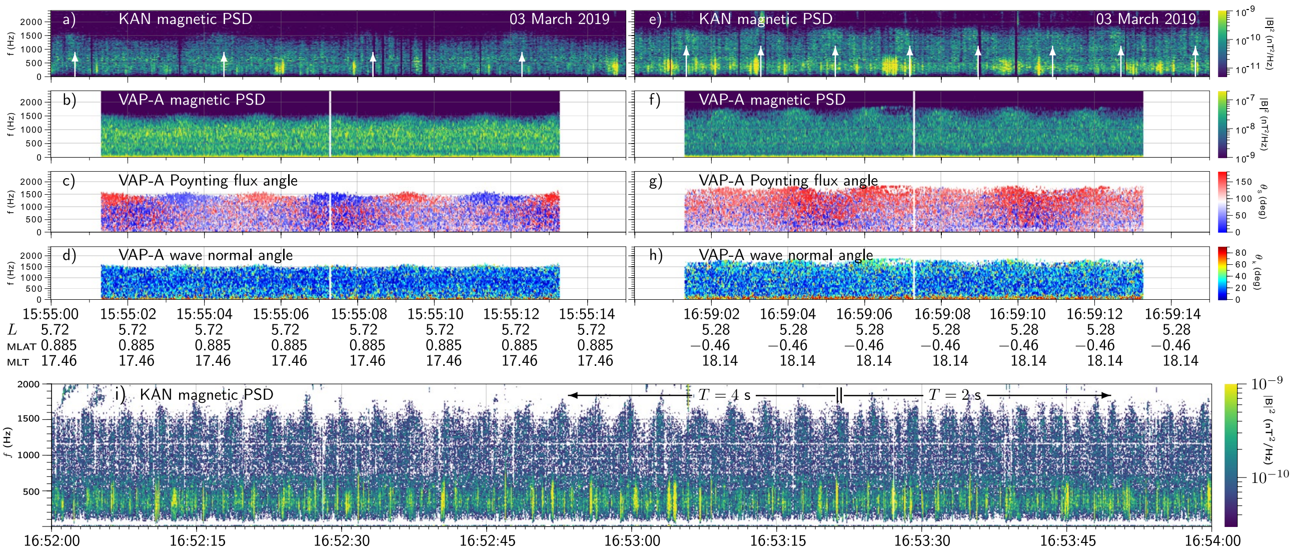

Figure 1. Spectrograms of periodic emissions (PEs) for two 15-s intervals at Kannuslehto (KAN) ((a and e), magnetic power spectral density (PSD)) and Van Allen Probe A (VAP-A): (b and f) magnetic PSD, (c and g) Poynting flux polar angle θ_S, and (d and h) wave normal angle θ_k. (i) Magnetic PSD at KAN for a 2-min interval. White arrows on panels (a and e) show power peaks at KAN.

The event comprised two parts with different characteristics. Part 1 lasted from 15:51 to 16:53 UT. Figures 1a–1h show the spectrograms for two intervals near the beginning and the end of the event belonging to part 1 and part 2, respectively. A longer (2-min) interval for KAN is shown in Figure 1i. The spectra at LOZ are quite similar to those at KAN. Using singular value decomposition (SVD) technique (Santolík et al., 2003), we found that the waves at VAP-A were right-hand circularly polarized (not shown) and had fairly low (i.e., far from the resonance cone and below the Gendrin angle) wave normal angles to the geomagnetic field (Figures 1d and 1h), that is, they were electromagnetic whistler mode waves. Wave normal angles varied within the range below 40° throughout the entire event but these variations were not related to the regime changes. The magnetic planarity (not shown) exceeded 0.5 most of the time, so the wave propagation analysis can be considered reliable.

At 15:55 UT, PEs are seen in the frequency range 1.2–1.7 kHz, on top of a hiss band that existed during the entire event both at KAN/LOZ and VAP-A. The power modulation period is $T \approx 4$ s at KAN and $T \approx 2$ s at VAP-A (Figures 1a and 1b). We determined the period by eye, dividing the time between the farthest peaks in each 12-s interval by the number of periods between them. The same procedures were used for VAP-A and KAN/LOZ for consistency. Fourier analysis of the spectral power envelope yielded the same results (not shown) but relative error was higher because of the small number of periods in each interval.

The spectra for part 2 that started at 16:53 UT are shown in Figures 1e–1f. The PE frequency and intensity became slightly higher, and the period was $T \approx 2$ s both at KAN and VAP-A.

The period change occurred sharply, as is seen in Figure 1i. The first additional peak with 2-s interval appeared between the peaks at 16:53:21 and 16:53:25.

3.2. Wave Propagation Directions Onboard VAP-A

Figures 1c and 1g show the Poynting flux polar angles θ_S for VAP-A observations. The neighboring pulses at VAP-A have clearly opposite propagation directions at 15:55 UT (Figure 1c). The same is true for the entire time interval till 16:53 UT. If we select only pulses propagating in one direction, then the period at VAP-A coincides with that at KAN.

At 16:59 UT (Figure 1f), when the PE power modulation periods at VAP-A and KAN are the same, the Poynting flux at VAP-A has one dominant direction corresponding to southward propagation in all pulses. This direction is away from the geomagnetic equator, since VAP-A was at MLAT = −0.46° at that time.

10.1029/2021GL095476

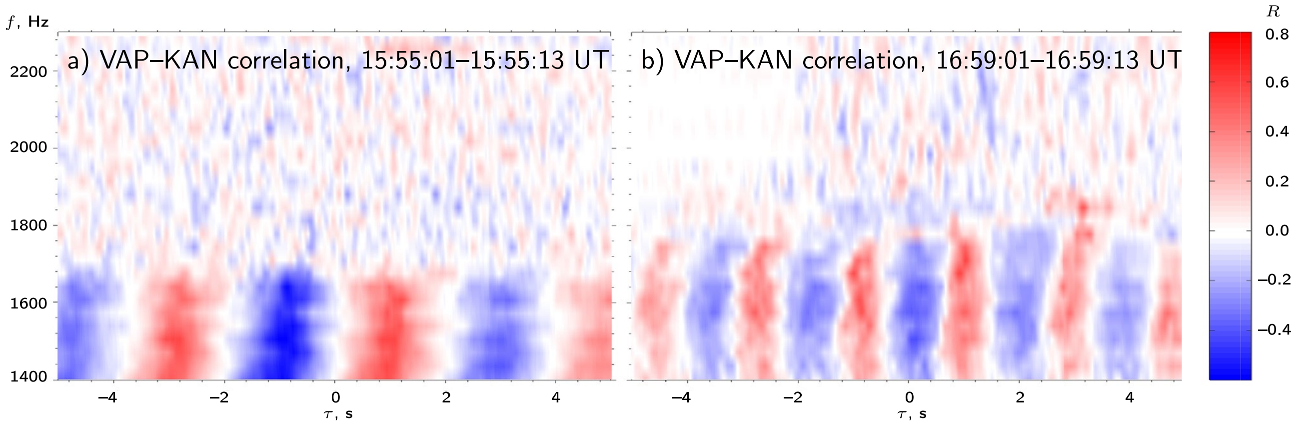

Figure 2. Correlation coefficient between the magnetic power spectral density (PSD) at Van Allen Probe A (VAP-A) and Kannuslehto (KAN) for the time intervals shown in Figures 1a–1d (a) and Figures 1e–1h (b). The PSD at VAP-A was multiplied by ± 1 for Poynting flux directed from/to KAN.

The hiss at frequencies below PE does not show a dominant propagation direction during both intervals.

3.3. Time Delay Between PE Observed on the Ground and RBSP-A

Figure 2 shows the correlation coefficient R between the pulses observed at VAP-A and KAN taking into account the propagation direction of waves at VAP-A. It was calculated after multiplying the magnetic field power spectral density by $-\operatorname{sgn}(\cos\theta_S)$. Therefore, positive correlation for power maxima indicates propagation away from KAN ($\theta_S = 180°$) and anticorrelation indicates propagation toward KAN ($\theta_S = 0°$).

In Figure 2a, the interval between positive maxima of R is ~4 s, corresponding to the pulse repetition period at KAN. The maximum at $\tau \simeq 1$ s corresponds to the pulses detected first at KAN and then propagating to VAP-A. The negative minimum at $\tau \simeq -1$ s corresponds to the pulses detected first at VAP-A and propagating toward KAN. The absolute delay values for these maximum and minimum are the same (1 s), that is consistent with the same propagation path.

In Figure 2b, the interval between positive maxima of R is about ~2 s and also equal to the repetition period at KAN that halved by that time. The first maximum with positive delay τ remains at 1 s that implies the same propagation path from KAN to VAP-A as earlier. Recall that the propagation direction at VAP-A is not alternating in this case (Figure 1g). Therefore, unlike Figure 2a, correlated wave packets (i.e., the power maxima) always correspond to positive R. The anticorrelation (negative R) occurs in this case when a maximum amplitude at VAP-A corresponds to a minimum at KAN.

3.4. Wave Propagation Directions on the Ground

The geomagnetic projection of VAP-A orbit to the Northern ionosphere is shown in Figure 3a. We used two-component measurements at KAN to calculate the angle α of the polarization ellipse minor axis (Figure 3b). Three-component measurements at LOZ allow us to obtain the directions of VLF wave Poynting flux on the ground. More precisely, we calculate the azimuthal angle α_S of the direction opposite to the Poynting flux (backazimuth) counted from north. These angles are shown in Figure 3c. No clear preference of a single propagation direction is obvious from Figures 3b and 3c, so we constructed distributions of the Poynting flux backazimuth in the frequency range of 1,400–1,700 Hz where the PEs were observed. We filtered out the odd power-line harmonics in the frequency ranges $f = 50 * (2n - 1) \pm 2$ Hz having a great power level and thus masking natural emissions in the direction distributions. The data in a moving time window (0.5 s) were binned according to the propagation angle, and the total Poynting flux corresponding to every bin was calculated. These results are shown in Figures 3d and 3e. A preferential south-west direction ($\alpha_S \approx 135°$) can be seen during the entire event. However, one also easily identifies another direction ($\alpha_S \approx 315°$), corresponding to the waves propagating from north-east. This second direction becomes more

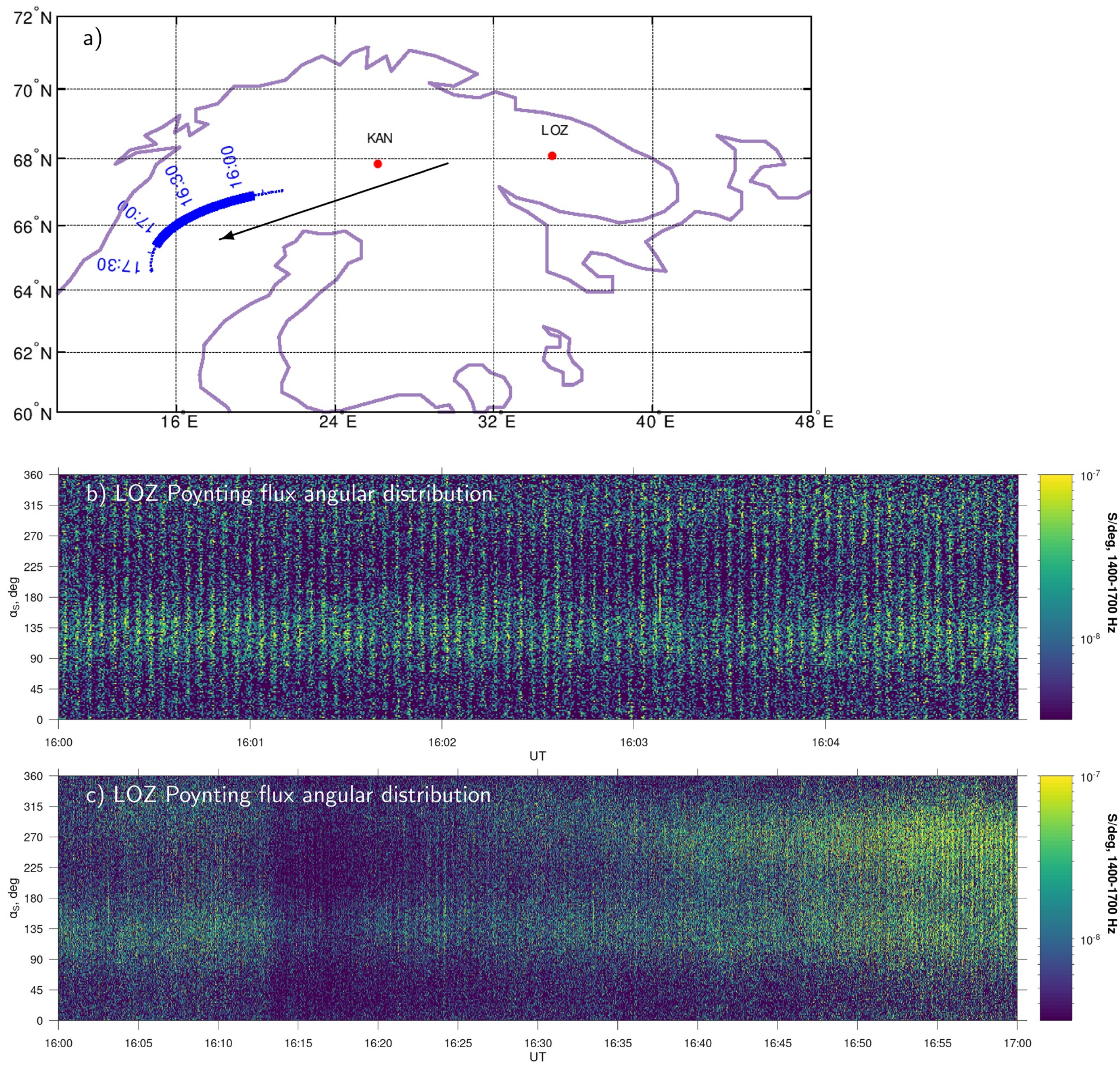

Figure 3. (a) Geomagnetic projection of the Van Allen Probe A (VAP-A) orbit on the map. The trajectory part where periodic emissions were observed is marked by a thick segment, an arrow shows approximate south-east direction. (b and c) Poynting flux distributions over the propagation angles at Lovozero (LOZ) for shorter and longer time interval, respectively.

prominent since 16:40 UT, and the corresponding maximum is shifted to $\alpha_S \approx 270°$. However, the period change at 16:53:20 UT is not associated with a sharp redistribution over the propagation directions.

Note that the scales in Figures 3d and 3e are absolute, that is, one can see the wave intensity variations. In particular, the intensity decreased from 16:13 to 16:20 UT, and additional increase is seen after 16:40 UT.

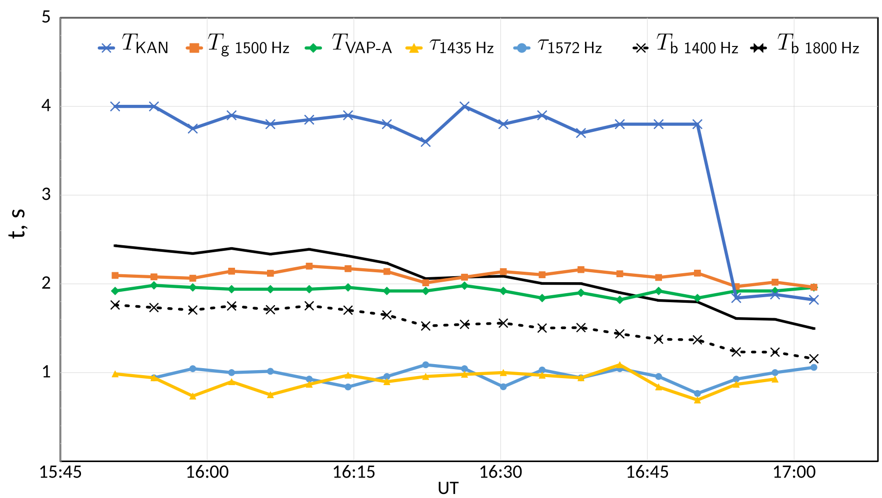

Figure 4. Characteristic timescales related to the periodic emission (PE) event: repetition periods of PE at KAN (T_{KAN}) and Van Allen Probe A (VAP-A; T_{VAP}), one-hop whistler-mode time $T_{g1500\,Hz}$, delay τ of the signal at VAP-A with respect to Kannuslehto (KAN) at 1,435 and 1,572 Hz, and one half of bounce periods of electrons with parallel energies corresponding to the cyclotron resonance at 1,400 and 1,800 Hz.

4. Discussion

4.1. Space-Time Structure of the VLF Waves in PEs

Figure 4 shows periods of PE at KAN and VAP-A plotted by using the intervals of simultaneously available data. The period of $T \approx 4$ s was constant at KAN since the start of PE observations for almost 1.5 h. During that time, the Poynting flux direction at VAP-A was alternating from pulse to pulse. At 16:53 UT, the period at KAN sharply decreased twofold. This period of 2 s was observed for 12 min, to 17:05 UT, that is, till the end of this event. The power modulation period at VAP-A was about 2 s during the entire observation interval.

We calculated the one-hop times T_g assuming field-aligned propagation of whistler-mode waves and using plasma density and magnetic field measured by VAP-A. A gyrotropic ($N_e \propto |\vec{B}|$) distribution of electron density N_e along the geomagnetic field $\vec{B}$ was assumed, and a dipole $\vec{B}$ model was used. These results for $f = 1500$ Hz are also shown in Figure 4. The calculated group propagation time is in good agreement with the power repetition period at VAP-A and exceeds twice the measured time delay of 1 s between KAN and VAP-A.

Taking into account that VAP-A was very close to the equator, the delays of 1 s between VAP-A and KAN measured during the first part of the event, imply the one-hop time of ≃2 s, that is, close to the calculated value. The two-hop time is ≃4 s, that is, equal to the repetition period at KAN. Therefore, both the dynamic spectra of VLF waves at KAN and VAP-A (Figures 1a–1c) and the structure of ground-spacecraft correlation coefficient R (Figure 2a) correspond to a single wave packet oscillating back and forth along a magnetic flux tube.

After the change at 16:53 UT, the period is equal to T_g both at KAN and VAP-A. This can naturally be explained by the existence of two whistler-mode wave packets propagating almost symmetrically between the hemispheres. These wave packets meet at the equator, and the period there remains equal to T_g. If the powers of these wave packets were equal, then the Poynting flux would not have had a predominant direction. In the opposite case, the direction of the wave packet with higher amplitude prevails.

The latter variant is most probably realized in our case, since the Poynting flux is directed southward in all pulses at VAP-A (Figure 1g). This scheme is the only one we can propose to satisfy all observed facts. It explains the positive maximum of R at the negative delay $\tau \approx -1$ s in Figure 2b. This delay, equal to the half-hop time, corresponds to the northward propagating pulses reaching KAN, but these pulses are not seen at VAP-A since they are hidden behind the southward propagating pulses having higher amplitudes. The positive sign of R agrees well with the prevalence of southward propagating pulses (recall that the power was multiplied by $-\operatorname{sgn}(\cos\theta_S)$ when calculating R).

The discussed scheme does not require the exact similarity of the counter propagating wave packets. It also works well if the weaker wave packet has a shorter duration that can be due to its lower excess over the detector noise background. Note that Figure 1g shows some evidence of oppositely (northward) propagating waves near the edges of stronger wave packets. In particular, it is clearly seen at 16:59:04.3 and 16:59:08 UT at the top of the wave packets and at 16:59:09 at the side of the starting wave packet.

4.2. Possible Location of PE Emission Source

Periodic emissions reported above had similar spectra on the ground and onboard VAP-A, and there was a stable time delay during the entire interval of conjugate observations. The period halving at KAN coincided with the change in Poynting flux variation at VAP-A from alternating to one-directional. These facts suggest a common source of the signals observed at KAN and VAP-A.

The preferential south-west direction ($\alpha \approx 135°$) that is seen on the angular distribution maps in Figures 3c and 3d is close to the magnetic projection of the VAP-A trajectory to the ground, which allows us to assume that VAP-A could have passed the source region at the time of the event. This assumption seems to agree with long-term PE detection onboard VAP-A and with the fact that the observed time delays between the waves at VAP-A and KAN were consistent with the field-aligned propagation of whistler mode waves.

PE started somewhat later at VAP-A (15:51 UT) than at KAN and LOZ (15:35 UT), and during that time VAP-A moved along the same $L = 5.9$. We can speculate that VAP-A reached a source flux tube at 15:55. Later on VAP-A observed the PE till 17:07 UT when it was at $L = 5.6$, and the event stopped simultaneously both at KAN and VAP-A.

The presence of the other preferred azimuth of wave propagation at LOZ that is obvious in Figure 3d is difficult to explain in any other way than by assuming that the ducted waves occupying the source flux tube (passed by or close to VAP-A) could also propagate in some other directions after their reflections from the ionosphere and thus spread across the geomagnetic field. Similar spreading could also occur if some waves leave the ducted regime and are reflected from the lower-hybrid resonance region (Shklyar & Jiříček, 2000).

Overall, the propagation direction on the ground was not very clear (Figures 3b–3d), which could indicate a fairly close location of the region of wave propagation to the ground to KAN and LOZ. This is consistent with the fact that the polarization at KAN and LOZ (not shown) was right-handed during the event. We do not know the actual extent of the source region, so we may speculate that it could be extended in longitude and thus occupy the flux tubes closer to KAN and LOZ than those crossed by VAP-A. However, an extended source implies rather high synchronization of wave generation over a large area, which may be problematic to explain theoretically.

4.3. Possible Generation Mechanisms

Taking into account long event duration, it is obvious that the wave packet energy losses at each hop were compensated by cyclotron amplification in the equatorial region (Trakhtengerts & Rycroft, 2008). A large number of hops implies ducted propagation in the magnetosphere, which is consistent with the observed and calculated ground–spacecraft delays. Ducting seems to require density inhomogeneities and such ducts were observed earlier (Demekhov et al., 2020; Koons, 1989). They were not detected by VAP-A in this event. However, shallow ducts with density variation below 10% and thus not detectable by the VAP-A instruments (Kurth et al., 2015) could exist. Possible ducting role of such small inhomogeneities was discussed by Hanzelka and Santolík (2019).

The dispersion-related difference in T_g between the lower and upper PE frequencies (1,400 and 1,700 Hz) reaches 0.1 s (not shown). Therefore, the persistent dynamic spectrum of subsequent pulses requires a nonlinear factor that compensates for the group velocity dispersion. This stable shape distinguishes the PE from multi-hop whistlers for which the dispersion effect is accumulated from pulse to pulse.

A model based on quasi-linear modification of the energetic electron distribution function by the generated waves was proposed by Bespalov (1984). This model in general complies with a hypothesis suggested by Helliwell (1963, and 1965) that each previous element excites the next one. However, a self-consistent nature of this process is stressed in the model. The generation of pulses with repeating dynamic spectrum is similar to passive mode locking in masers and lasers, which is a specific form of mode competition. In this case, each pulse modifies the distribution function in such a way that only those portions of the reflected pulse that match the primary pulse are amplified on the next hop, while the dispersed portions are damped.

According to this model, the pulse repetition period on the ground can be $2T_g/n$, where n is integer. The longest period corresponds to a single pulse bouncing back and forth between the conjugate ionospheres. This case corresponds to the beginning of our event.

A sharp halving of the repetition period on the ground can be related to a change in the generation regime in the magnetospheric cyclotron maser. This change could be caused by a variation in either energetic particle population in the generation region or the VLF wave reflection in one or both hemispheres. We did not notice any strong changes in the energetic particle population detected by VAP-A. Therefore, if the spacecraft crossed the source region during PE observations, the change in the generation regime was probably related to the ionospheric reflection change. Indeed, the local time of the event approximately corresponded to the solar terminator passing.

Another factor that could be related to the generation regime change is an increase in the wave power that is evident from ground-based observations (Figure 3e). We cannot say whether this increase is caused by magnetospheric conditions or ionospheric reflection but, in its turn, it can influence the ionospheric reflection by precipitating electron flux (Villalon et al., 1989).

A good agreement between the calculated one-hop whistler time and the pulse period, as well as the sharp halving of the repetition period speak in favor of the passive mode locking regime. On the other hand, quantitative development of this model was done by using bounce-averaged equation for the energetic electron distribution function. Calculated bounce times for the low pitch-angle resonant electrons shown in Figure 4 are close to the wave hop times. Therefore, the model of Bespalov (1984); and Bespalov et al. (2010) requires an improvement taking into account bounce resonance effects in order to be quantitatively applicable for the reported event. Recall that the idea to relate PE period with the electron bounce period was suggested by Dowden (1962).

5. Conclusions

In summary, we have observed periodic VLF emissions at VAP-A and ground-based stations KAN and LOZ. To our knowledge, this is the first report on conjugate observation of PEs in the near-equatorial magnetosphere and on the ground, although this emission type is well-known since the 1960s from ground-based observations. The similarity of dynamic spectra of individual pulses for the entire event lasting more than an hour distinguishes PEs from multi-hop whistlers. The repetition period on the ground was 4 s in the first part of the event, and it halved sharply for the second part, while the power repetition period onboard VAP-A was 2 s during the entire event. These periods and delays between the wave pulses detected on the ground and by VAP-A are consistent with field-aligned propagation of whistler mode waves. Halving of the repetition period corresponded to a change from the regime with a single-wave packet bouncing back and forth along the field line to the other regime, with two wave packets propagating symmetrically in time that syhcnronously meet at the equator. The Poynting flux direction remained the same in the second regime, which implies that one of the two wave packets had slightly higher amplitude. Both observed regimes are consistent with a model of passive mode locking in the magnetosphere whistler-mode cyclotron maser, and a sharp transition from one regime to the other could occur to the change in the ionospheric reflection of VLF waves related to the terminator crossing.

Data Availability Statement

VAP-A data used in this paper can be found on the EMFISIS website (http://emfisis.physics.uiowa.edu/Flight/). KAN data are available at https://www.sgo.fi/pub_vlf/VLFPlots2019/2019_03/Kannuslehto20190303_1min_16kHz/. LOZ data are available at http://aurora.pgia.ru:8071/index.php?p=1&s=2&x=MMLZ&t=1551571200.

Acknowledgments

The work of A. G. Demekhov, E. E. Titova, A. S. Nikitenko, and S. V. Pilgaev was partially supported by the State task AAAA–A18–118012490100–7 of Polar Geophysical Institute. The work with KAN data was supported by the Academy of Finland under grant 330783. The authors would like to thank the designers of Van Allen Probes and developers of the instruments (EMFISIS—Craig Kletzing) for the open access to the data.

References

Bespalov, P. A. (1984). Passive mode locking in masers with unequally spaced spectra. *Soviet Physics Journal of Experimental and Theoretical Physics*, *60*(6), 1090–1095.

Bespalov, P. A., Parrot, M., & Manninen, J. (2010). Short-period VLF emissions as solitary envelope waves in a magnetospheric plasma maser. *Annales Geophysicae*, *72*, 1275–1281. https://doi.org/10.1016/j.jastp.2010.09.001

Demekhov, A. G., Titova, E. E., Maninnen, J., Pasmanik, D. L., Lubchich, A. A., Santolík, O., et al. (2020). Localization of the source of quasiperiodic VLF emissions in the magnetosphere by using simultaneous ground and space observations: A case study. *Journal of Geophysical Research: Space Physics*, *125*(5), e2020JA027776. https://doi.org/10.1029/2020JA027776

Dowden, R. L. (1962). Very-low-frequency discrete emissions received at conjugate points. *Nature*, *195*, 64–64. https://doi.org/10.1038/195064a0

Engebretson, M. J., Posch, J. L., Halford, A. J., Shelburne, G. A., Smith, A. J., Spasojevic, M., & Arnoldy, R. L. (2004). Latitudinal and seasonal variations of quasiperiodic and periodic VLF emissions in the outer magnetosphere. *Journal of Geophysical Research*, *109*(A05), A05216. https://doi.org/10.1029/2003JA010335

Fedorenko, Y., Tereshchenko, E., Pilgaev, S., Grigoryev, V., & Blagoveshchenskaya, N. (2014). Polarization of ELF waves generated during "beat-wave" heating experiment near cutoff frequency of the Earth-ionosphere waveguide. *Radio Science*, *49*(12), 1254–1264. https://doi.org/10.1002/2013RS005336

Hanzelka, M., & Santolík, O. (2019). Effects of ducting on whistler mode chorus or exohiss in the outer radiation belt. *Geophysical Research Letters*, *46*(11), 5735–5745. https://doi.org/10.1029/2019gl083115

Helliwell, R. A. (1963). Whistler-triggered periodic very-low-frequency emissions. *Journal of Geophysical Research*, *68*(19), 5387–5395. https://doi.org/10.1029/j.2156-2202.1963.tb00019.x

Helliwell, R. A. (1965). *Whistlers and related ionospheric phenomena*. Stanford University Press.

Helliwell, R. A., & Brice, N. (1964). Very low frequency emission periods and whistler-mode group delays. *Journal of Geophysical Research*, *69*, 4704–4708. https://doi.org/10.1029/JZ069i021p04704

Kletzing, C. A., Kurth, W. S., Acuna, M., MacDowall, R. J., Torbert, R. B., Averkamp, T., et al. (2013). The electric and magnetic field instrument suite and integrated science (EMFISIS) on RBSP. *Space Science Reviews*, *179*(1), 127–181. https://doi.org/10.1007/s11214-013-9993-6

Koons, H. C. (1989). Observations of large-amplitude, whistler-mode wave ducts in the outer plasmasphere. *Journal of Geophysical Research*, *94*(A11), 15393–15397. https://doi.org/10.1029/ja094ia11p15393

Kurth, W. S., De Pascuale, S., Faden, J. B., Kletzing, C. A., Hospodarsky, G. B., Thaller, S., & Wygant, J. R. (2015). Electron densities inferred from plasma wave spectra obtained by the Waves instrument on Van Allen Probes. *Journal of Geophysical Research: Space Physics*, *120*, 904–914. https://doi.org/10.1002/2014JA020857

Lokken, J. E., Shand, J. A., Wright, C. S., Martin, L. H., Brice, N. M., & Helliwell, R. A. (1961). Stanford–Pacific naval laboratory conjugate point experiment. *Nature*, *192*, 319–321. https://doi.org/10.1038/192319b0

Manninen, J. (2005). Doctoral dissertation *Some aspects of ELF-VLF emissions in geophysical research*. Sodankylä Geophysical Observatory Publications. Retrieved from http://www.sgo.fi/Publications/SGO/thesis/ManninenJyrki.pdf

Manninen, J., Demekhov, A. G., Titova, E. E., Kozlovsky, A. E., & Pasmanik, D. L. (2014). Quasiperiodic VLF emissions with short-period modulation and their relationship to whistlers: A case study. *Journal of Geophysical Research*, *119*(A6), 3544–3557. https://doi.org/10.1002/2013JA019743

Mauk, B. H., Fox, N. J., Kanekal, S. G., Kessel, R. L., Sibeck, D. G., & Ukhorskiy, A. (2012). Science objectives and rationale for the radiation belt storm probes mission. *Space Science Reviews*, *179*, 3–27. https://doi.org/10.1007/s11214-012-9908-y

Santolík, O., Parrot, M., & Lefeuvre, F. (2003). Singular value decomposition methods for wave propagation analysis. *Radio Science*, *38*(1), 1010. https://doi.org/10.1029/2002JA009791

Shklyar, D., & Jiříček, F. (2000). Simulation of nonducted whistler spectrograms observed aboard the MAGION 4 and 5 satellites. *Journal of Atmospheric and Solar-Terrestrial Physics*, *62*(5), 347–370. https://doi.org/10.1016/s1364-6826(99)00097-8

Trakhtengerts, V. Y., & Rycroft, M. J. (2008). *Whistler and Alfvén mode cyclotron masers in space*. Cambridge University Press.

Villalon, E., Burke, W. J., Rothwell, P. L., & Silevitch, M. B. (1989). Quasi-linear wave-particle interactions in the earth's radiation belts. *Journal of Geophysical Research*, *94*(A11), 15243–15256. https://doi.org/10.1029/ja094ia11p15243